Performance Characteristics of Brownian Motors

Heiner Linke,[1] Matthew T. Downton,[2] and Martin J. Zuckermann[2]

[1]*Materials Science Institute and Physics Department, University of Oregon, Eugene, OR, 97405, USA*

[2]*Department of Physics, Simon Fraser University, Burnaby, B.C. V5A 1S6, Canada*

(Dated: January 25, 2005)

Abstract

Brownian motors are non-equilibrium systems that rectify thermal fluctuations to achieve directed motion, using spatial or temporal asymmetry. We provide a tutorial introduction to this basic concept using the well-known example of a flashing ratchet, discussing the micro- to nanoscopic scale on which such motors can operate. Because of the crucial role of thermal noise, the characterization of the performance of Brownian motors must include their fluctuations, and we review suitable performance measures for motor coherency and efficiency. Specifically, we highlight that it is possible to determine the energy efficiency of Brownian motors by measuring their velocity fluctuations, without detailed knowledge of the motor function and its energy input. Finally, we exemplify these concepts using a model for an artificial single-molecule motor with internal degrees of freedom.

PACS numbers: 05.40.Ca, 05.40.Jc, 87.15.Ya

Keywords: Brownian motor, efficiency, Peclet number, fluctuations

When a machine becomes small enough, thermal fluctuations become large compared to the energies that drive the motor. Motors and machines that operate on the micro- and nanoscales therefore must at least tolerate their stochastic environment. Motor designs that actually incorporate thermal fluctuations into their function are called 'Brownian motors' and are thought to be essential to controlled motion at the nanoscale. Here we introduce the concept of Brownian motors.

The performance characteristics of motors working on the nanoscale are richer than those of macroscopic machines. Specifically, fluctuations of position and velocity are inherent to all Brownian motors, they affect the motor performance and they contain information about the motor characteristics. We review suitable criteria for the characterization of the performance of Brownian motors, and use the concept for an artificial single-molecular motor to illustrate how the motor design can influence the motor performance. As artificial nanomotors move into technological reach in areas as diverse as synthetic chemistry, nanoelectronics and nanofluidics, such considerations are becoming increasingly important.

I. INTRODUCTION: BROWNIAN MOTORS

A Brownian motor is a system that achieves directed motion by rectifying thermal fluctuations [1–5]. Usually, we mean by 'directed motion' quite literally the transport of particles, but the same idea applies to transport in some more abstract parameter space, such as a reaction coordinate. To illustrate the Brownian motor concept, we use the so-called 'flashing ratchet' [6–8] (also called 'pulsating ratchet' [4]), shown in figure 1. In this system, particles are subject to a spatially periodic, asymmetric potential, such that the time-dependent particle coordinate $x(t)$ is described by

$$m\ddot{x}(t) = -V'(x(t)) - \gamma\dot{x}(t) + \xi(t). \tag{1}$$

Here, $V(x)$ describes the 'ratchet' potential, which has a broken spatial symmetry, and is usually taken to be spatially periodic with period L, such that $V(x) = V(x + L)$. The term $\xi(t)$ is a zero-mean, delta-correlated, Gaussian white noise that describes the fluctuations imposed onto the particle by the interaction with a 'heat bath' at equilibrium temperature T. The term $\gamma\dot{x}(t)$, where γ is the drag coefficient, describes a frictional force experienced by the particle when it is moving relative to its environment. The drag term is in generic theoretical work usually assumed

to be linear in the velocity, in excellent agreement with many experimental realizations, such as colloidal particles in liquids [9–12], Josephson junctions [13–16], or magnetic flux quanta in superconductors [17–19] (note however, that other types of particles, such as non-equilibrium electrons in a semiconductor [20–22], may experience dissipation that is not linear in v). In many experimental realizations (including colloids) the characteristic time for momentum relaxation, given by (m/γ), is extremely short: for instance, for a spherical particle with diameter 100 nm in aqueous solution, $(m/\gamma) \approx 1$ ns. When (m/γ) is much smaller than any other relevant time scale of the system (overdamped limit), the inertial term can be neglected, and eqn. (1) becomes the Langevin equation

$$\gamma \dot{x}(t) = -V'(x(t)) + \xi(t). \tag{2}$$

In this limit, the particles' velocity is in every instant given by $v = F_{\rm net}/\gamma$, where $F_{\rm net}$ is the sum of all forces applied to the particle in that instant (including noise). Both $\xi(t)$ and γ are determined by the interaction of the particle with the molecules in its environment, and are thus related to one another by the fluctuation-dissipation relation [5, 23–25]

$$\langle \xi(t)\xi(s) \rangle = 2\gamma kT\delta(t-s). \tag{3}$$

In the presence of thermal noise as defined in eqn. (3), the particles' diffusion constant D is given by the Einstein relation, $D = kT/\gamma$. For a spherical object in a fluid with viscosity η, the drag coefficient is given by Stokes' law, $\gamma = 6\pi\eta r$. Equation (2) describes the overdamped particle system in thermal equilibrium. Crucially, regardless of the potential's symmetry, detailed balance is valid, that is, the probability for a particle to make a thermally activated transition from x to, say, $(x + \Delta x)$ equals the probability for the reverse step from $(x + \Delta x)$ to x, for arbitrary x and Δx. Clearly, then, no net transport can be observed in thermal equilibrium.

To turn a system as described in eqns. (1) or (2) into a Brownian *motor*, one needs to break detailed balance by driving the system away from thermal equilibrium. One way of doing so is to introduce a time-dependence into the potential, for instance of the form $V(x,t) = \Theta(t)V(x(t))$. In the simplest case, $\Theta(t)$ is dichotomous and switches between the value $\Theta(t) = 1$, where the potential is 'on' (see fig. 1), and the value $\Theta(t) = 0$, where the potential is flat ('off' in fig. 1).

Crucially, the process of keeping a system away from thermal equilibrium (in the present example by cyclic 'flashing' of the ratchet potential) requires input of free energy. Therefore, the particle transport that normally [4, 5] occurs in such a non-equilibrium situation does *not* violate the Second Law of Thermodynamics, which applies to equilibrium situations without net flow of free energy.

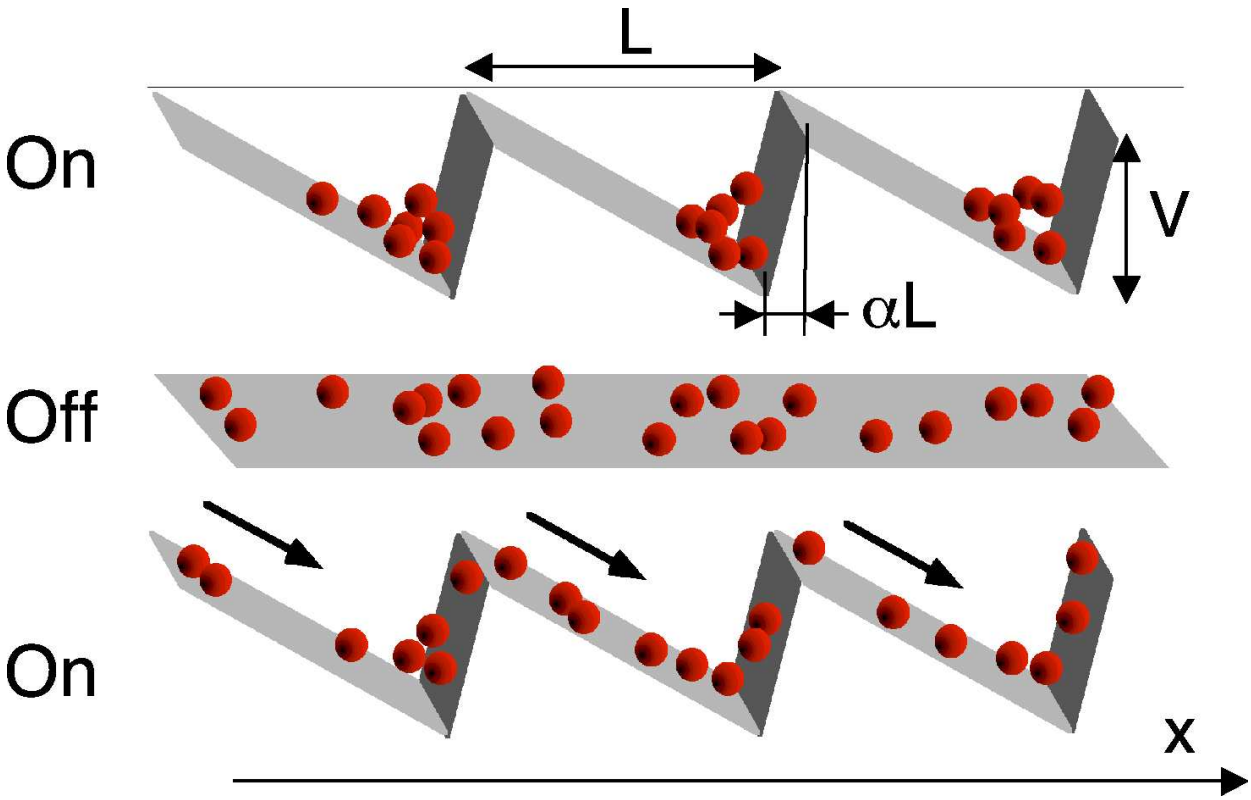

FIG. 1: A flashing ratchet switches between an on- and an off-state. During the on-phase, Brownian particles concentrate around the potential minima. During the off-phase, the particles undergo one-dimensional, isotropic diffusion. Periodic or stochastic switching between the two states induces a particle current in positive x-direction. For an illustrative Java applet, see [26].

Suppose the potential in fig. 1 is off at first, such that particles are on average evenly distributed in space. If the potential is switched on, particles will during a transient period of time move toward the closest local potential minimum. Due to the asymmetry of the potential, the nearest accessible minimum is on average to the right of the particle. Consequently, the particle distribution shifts to the right. On the other hand, when the potential is switched off, the particles spread out isotropically on average, and no overall shift of the particle distribution occurs. Consequently then, periodic or stochastic switching of the potential results in a net particle flow in positive x-direction (for an illustrative Java applet, see [26]).

The operation of the flashing ratchet as described above can be substantially modified [4]: for instance, the Brownian motor effect is observed for periodic as well as for random fluctuations of the potential (where the potential does not necessarily need to switch between fully on and fully off) [8], for modified potential shapes, in the presence of finite inertia, and when the cycling of the potential is replaced by a cycling of temperature [4, 27]. The flashing ratchet has also been

proposed as a model for linear molecular motors, such as the transporter molecule kinesin which exhibits directional motion along microtubules in the presence of a non-equilibrium concentration of ATP. For instance, one may interprete the polar, periodic microtubule as a 'ratchet' potential, to which the kinesin motor binds tightly during one stage of the ATPase cycle, while it remains losely bound, and able to perform one-dimensional diffusion along the microtubule, in another stage of the cycle [2].

Motor action in the strictest sense is defined as work W being performed against a conservative 'load' force F. The Langevin equation for such a motor reads

$$\gamma \dot{x}(t) = -\Theta(t)V'(x(t)) + F + \xi(t). \tag{4}$$

When the parameters are well-chosen, the current can flow against a small external force $F < 0$, such that the motor does work at the rate $P = \mathrm{d}W/\mathrm{d}t = F\langle v \rangle$ per particle, where $\langle v \rangle$ is the time average of the particle velocity, which normally increases monotonically as a function of F and goes through zero at what is defined as the stall force F_{stall}. A cartoon plot of $\langle v \rangle$ as a function of F for a Brownian motor (a so-called load-velocity curve) is shown in fig. 2. In the interval $F = [F_{\mathrm{stall}}, 0]$, the motor does work against the external load, which is, in principle, stored as potential energy and can be recovered later.

A. Speed of a flashing ratchet

To estimate the particle current in a flashing ratchet we follow [7, 12] and assume that, initially, the particles are perfectly localized in the potential minima (which means that the height of the potential barriers, V, is much larger than kT). We also assume that the transitions between the on- and off-states take place on a time scale that is much shorter than the times $T_{\mathrm{on}}$and T_{off}, during which the potential is on and off respectively, such that transients can be neglected. We focus our discussion on the particles in one potential minimum located at $x = 0$, and let the potential be switched off for a time interval T_{off}, during which the particles undergo one-dimensional Brownian motion. The resulting probability distribution for the position of a particle at the end of T_{off} is given by

$$p(x, T_{\mathrm{off}}) = \frac{\exp(-x^2/4DT_{\mathrm{off}})}{\sqrt{4\pi D T_{\mathrm{off}}}}. \tag{5}$$

In order to achieve transport, one needs to choose T_{off} sufficiently long such that the particles can diffuse the short distance (αL) between a potential minimum and a maximum (see fig. 1),

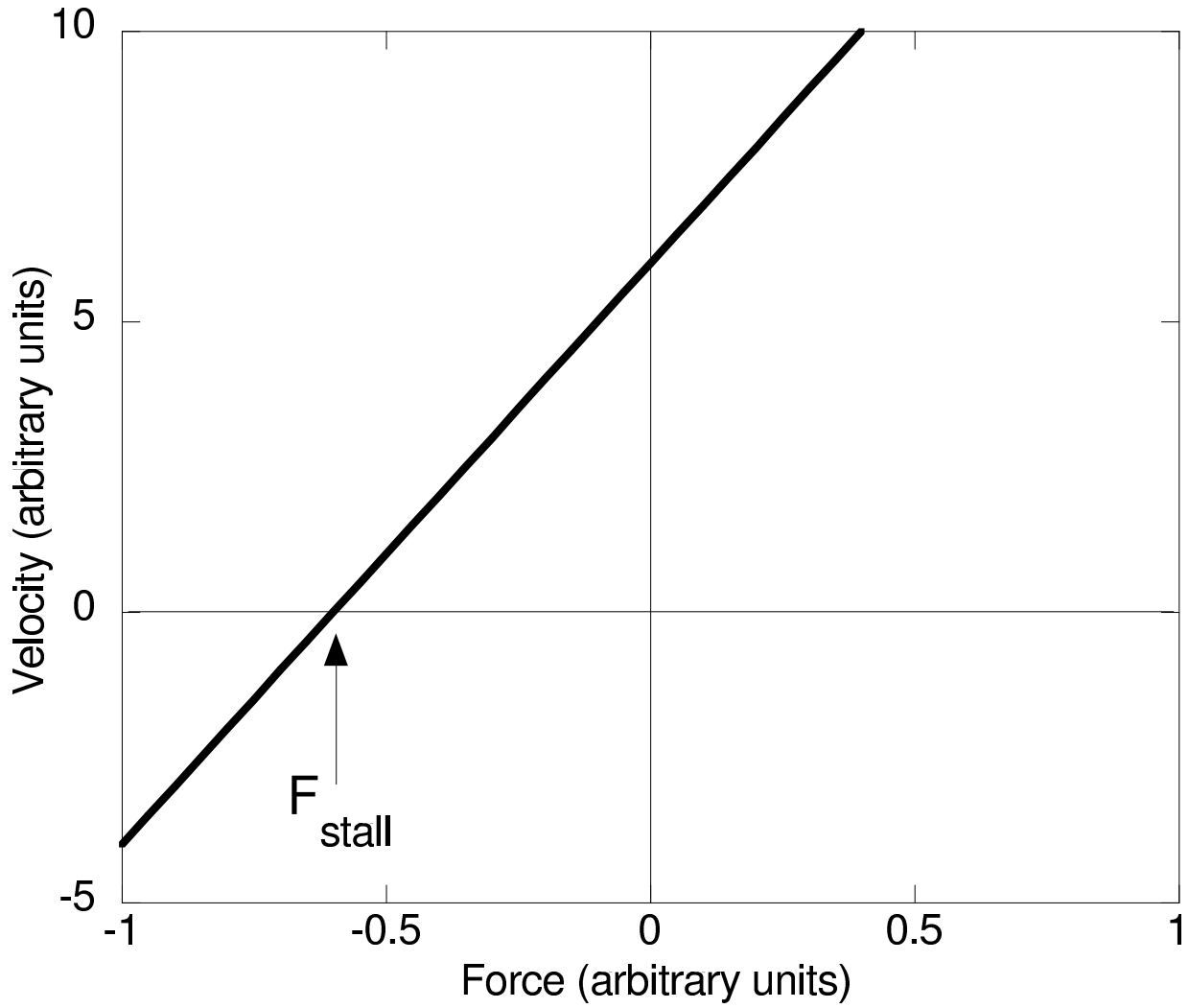

FIG. 2: Cartoon of a typical load-velocity curve of a Brownian motor in the presence of a load force. Without load force, the motor has a positive average velocity, while the motor moves backward when an excessive, negative force is applied. The stall force is the (negative) force at which the motor has zero velocity on average. Note that details of the force-velocity curve can look quite different from the cartoon shown here, including non-linear behavior. In general, the motor velocity in response to a positive force can even be negative (negative absolute mobility [28–30]).

but short enough to avoid substantial back-diffusion over the long distance, $(1-\alpha)L$, that is $(\alpha L)^2/2D \approx T_{\rm off} << (1-\alpha)^2 L^2/2D$. This condition can be fulfilled when $\alpha << 1$. The fraction of particles that will be transported to the left is then negligible, and the fraction, s, of particles that will be transported by one period L to the right is given by integrating p from αL to infinity

[7, 12]:

$$s = \frac{1}{2}\mathrm{erfc}(\alpha L/\sqrt{4DT_{\mathrm{off}}}) \tag{6}$$

where erfc is the complementary error function. For the choice $T_{\mathrm{off}} = (\alpha L)^2/2D$, one finds $s = \frac{1}{2}\mathrm{erfc}(\frac{1}{\sqrt{2}}) \approx 0.16$.

A good choice for the time T_{on} is given by the time it takes to completely localize all particles after the potential is switched on at the end of T_{off}. The time it takes a particle with drag coefficient γ to drift the distance $(1-\alpha)L$ under the influence of a force $V/(1-\alpha)L$ yields $T_{\mathrm{on}} = \gamma((1-\alpha)L)^2/V$.

During each full cycle of the flashing potential, the particle distribution shifts to the right by a distance sL, and the time-averaged, steady-state particle velocity is given by $\langle v\rangle = sL/(T_{\mathrm{on}}+T_{\mathrm{off}})$.

We emphasize that the estimates given above are an upper limit, which can be achieved only when $\alpha << 1$ and $V >> kT$, both of which can be difficult to obtain in experiments. For finite α, there will always be a finite amount of back-diffusion during T_{off}. When V is not much larger than kT, then the particle distribution at the end of T_{on} will not be perfectly localized at the potential minimum, but will be skewed towards the shallower confinement slope, effectively increasing the distance the particles have to diffuse during T_{off}. Both of these effects decrease the particle flux.

The central role of Brownian motion in this transport process implies that macroscopic motors cannot be constructed in this way. What is the upper limit for the particle size that can be effectively transported by a flashing ratchet? Because of the practical relevance of this question, we explore it with a real system in mind. Specifically, we assume that our particles are spherical with radius r, are colloidal in a fluid with viscosity η, and have a Stokes drag coefficient $\gamma = 6\pi\eta r$. In the following we consider the particle flux as a function of particle size in a ratchet whose period $L = 20r$ scales with the particle size. Furthermore, we use $V = 20kT$ and $\alpha = 0.1$ and set $T_{\mathrm{off}} = \alpha^2 L^2/2D$ such that $s \approx 0.16$ (see above). Using $T_{\mathrm{on}} = \gamma((1-\alpha)L)^2/V$ the average particle velocity as a function of the particle radius then becomes

$$\langle v\rangle = A\frac{kT}{\eta r^2}, \tag{7}$$

where we used the Einstein relation $\gamma D = kT$, and where $A \approx s/6\pi$ is a dimensionless value of order 10^{-2} (see fig. 3 for absolute numbers). Crucially, the drift speed increases with temperature and falls off with the square of the particle size, as one would expect for a diffusion-limited transport process, dramatically highlighting that Brownian motors are operational only for microscopic sizes. In fig. 3 we show the resulting velocity in absolute numbers for an aqueous, colloidal system at room temperature. Also indicated is the speed at which a spherical particle of radius r moves a

distance corresponding to its own diameter, $2r$, in every second, in some sense corresponding to 'human-scale' speeds. Compared to this measure, our model Brownian motor is hopelessly slow for objects larger than 10μm, but surprisingly 'fast' for particle sizes smaller than about 1μm: given an optimized flashing ratchet, a particle of diameter 100nm can, in principle, drift almost 200 times its own size (19μm) in every second. Compared to a car, this speed corresponds to supersonic velocities. The fact that an overdamped object should be able to move this fast is not *in spite* of thermal fluctuations and the viscous drag associated with them, but due to smart *use* of thermal fluctuations.

B. Stall force

Also the stall force of a Brownian motor is limited by thermal processes. Consider a motor that needs to cover a distance d by free diffusion, in the presence of a load force F. In the case of a flashing ratchet $d = \alpha L$, that is, the distance the particles need to cover by diffusion during $T_{\rm off}$. In another system, such as a protein motor, d could be given by a spatial distance related to a conformational change, that needs to be achieved by thermal activation (that is, some change in a reaction coordinate with a spatial component). Effective transport is possible when the 'downhill' drift at velocity F/γ in the load force field during $T_{\rm off}$ does not exceed d. Taking $T_{\rm off} = d^2/2D$, this consideration yields an estimate for the stall force of

$$F_{\rm stall} = 2\frac{kT}{d}, \tag{8}$$

where we again used the Einstein relation $\gamma D = kT$. Remarkably, one finds that the force against which a Brownian motor can do work increases with temperature and with smaller size. Using $d = \alpha L$, $\alpha = 0.1$ and $L = 20r$ as above, we find $F_{\rm stall} \approx kT/r$ (see fig. 3). In this context it is instructive to note that at room temperature $kT \approx 4.1$ pN nm, such that pN emerge as a natural force scale for nanoscale motors that incorporate thermal motion into their function.

For instance, we can estimate that biological motor proteins, which are found to have a stall force of order 10 pN [31], can rely on unaided thermal diffusion only for distances of no more than 0.5 nm, about 10% of a typical periodic step size ($L \approx 5-10$nm [31–35]), while the bulk of the motion must be achieved in a way that does not rely solely on Brownian motion (for instance so called 'power strokes'). While the typical performance characteristics of biomolecular motors nicely agree with the framework of a flashing ratchet [2, 36], one cannot draw the conclusion that biological motors are in general well described by flashing ratchets. Full models for biological motors are certainly

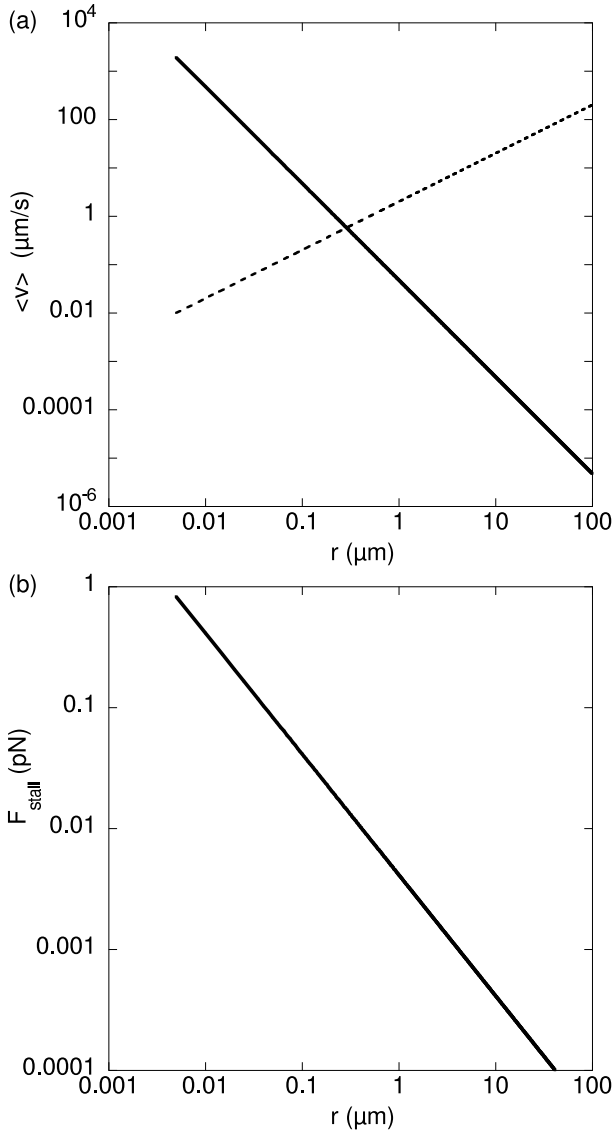

FIG. 3: (a) Estimate of the optimal velocity (full line) of a spherical particle in aqueous solution ($\eta = 10^{-3}$ Pa s, T = 300 K) in a flashing ratchet ($\alpha = 0.1, V = 20kT, L = 20r$) as a function of particle radius. For comparison we show the speed at which the particle translocates a distance corresponding to its own diameter every second, that is, v=2r/second (dashed line). Using this speed as a criteria, a Brownian motor is "fast" for particles smaller than about 1μm, and very slow for particles larger than about 10μm. (b) Upper-limit estimate for the stall force in a flashing ratchet as a function of particle size (see text for details). Nanometer-scale particles can move against forces on the picoNewton scale.

much more complex [37], and the way thermal fluctuations enter the mechanism of motion of, say, myosin, is not yet fully understood.

C. Definition of a Brownian motor

P. Reimann and P. Hänggi [5] defined a set of characteristics for a Brownian motor, that we follow here, and all of which are illustrated by the flashing ratchet described above:

1. Thermal noise plays a central role in achieving transport. Without the Brownian motion during the 'off'-phase (that is, at $T = 0$, or for macroscopic objects), no net current occurs. In this sense, the fluctuating, external potential rectifies thermal fluctuations - the hallmark of a Brownian motor.

2. Symmetry is broken. In the present example, *spatial* symmetry is broken through the use of a potential without inversion symmetry. Instead, symmetry may also be broken by use of an unbiased, but skewed, external, time-dependent force (dynamical symmetry breaking) [38, 39], or due to spontaneous symmetry breaking [36, 40–42].

3. Except for the load force, all forces average to zero (in the present case, the average is to be taken in space; more generally, the spatial, temporal and ensemble averages are zero).

4. Detailed balance is broken (that is, the system is kept away from thermal equilibrium, usually at the price of sustained energy input).

5. Finally, the use of periodicity (spatial or temporal) is typical for Brownian motors, and is required for a clean definition of what constitutes 'transport' or 'work' in a Brownian system.

Note further the importance of dissipation. Without the friction (drag) term in eqn. (1), and in presence of the inertial term, the particles will already after one or two potential cycles have sufficient kinetic energy (picked up due to work input from outside) to move continuously to the left on average. Friction dissipates kinetic energy into heat, and a 'thermostat' is required to keep the temperature of the heat bath from rising due to the fluctuating potential.

The term 'Brownian motor' as defined above was first introduced by Bartussek and Hänggi in 1995 [43]. A term with very similar meaning is that of a 'ratchet', which emphasizes the idea of spatial asymmetry and periodicity. Many authors define a 'ratchet' in precisely the same way as the above definition of a Brownian motor, including the requirement for thermal noise to play an important role in the transport mechanism [4]. Other authors have used the term ratchet more broadly for a system in which a spatially periodic, asymmetric potential is used to generate motion, but not necessarily with crucial influence from thermal noise. However, the term Brownian motor

should certainly be reserved for systems whose performance or functionality depends on thermal fluctuations.

Research on Brownian motors has traditionally been driven by theoretical work, with experiments usually motivated and initiated by theoretical predictions. A large variety of ratchet systems have been investigated. In addition to the flashing ratchet described above, these include 'rocking ratchets' (where a zero-mean, time-dependent, macroscopic force is applied and used to 'rock' the ratchet potential) with [44–46] and without [47–49] inertia effects. Significantly, the inclusion of inertia is found to lead to chaotic behavior [44, 45]. Ratchets have also been investigated in the regime in which quantum effects play an important role (so called quantum ratchets) [46, 50–53], and were found to show qualitatively different behavior compared to their classical counterparts. Specifically, the current in a rocking, quantum ratchet can revert its direction as a function of temperature, as a result of a competition between thermally activated transport and quantum tunneling [50, 54]. Significant attention has also been paid to models for biological molecular motors based on Brownian motors [2, 36, 55, 56]. A number of authors have studied cooperative effects in coupled motors, and a wealth of novel phenomena has been predicted. Examples are the reversal of the current direction as a function of particle size and density in a rocking ratchet when steric hindrance of particles is considered [57], enhanced velocity of elastically coupled Brownian motors [58, 59], symmetry breaking, anomalous hysteresis and absolute negative mobility [41, 60–63]. The phenomenon of absolute negative mobility, which describes a system in which application of an external force induced transport in a direction opposite to the applied force, can also be observed in the absence of coupling effects [28, 29]. The status of the ratchet field in 2002, with an emphasis on theory, was surveyed by Peter Reimann in his excellent, comprehensive review [4], which cites more than 700 references, and was summarized in [5]. For another, more recent review, see [39].

On the experiment side, representative experiments carried out before 2002 are reviewed in a special issue of Applied Physics A [64]. Outstanding examples and more recent experiments include the first experimental realizations of flashing ratchets for colloidal particles [9, 65], which in fact can be used to separate DNA segments by their size [10, 12], and ratchets for electrons realized in both classical [66] and quantum [54, 67] regimes, with applications in high-frequency nanoelectronics [68] and in thermoelectrics [69–71]. Quantum ratchets have also been realized using vortices in Josephson junctions [16], and ratchet-type devices have successfully been used to move magnetic flux quanta in superconductors [19]. One of the most promising areas of application of ratchet effects is the fact that the current direction often depends quite subtly on details of the parameters chosen, which makes it possible to use ratchets to separate different types of particles, for instance

by their size. Experimental realizations of such devices include, in addition to the DNA separator mentioned above [12], a microfluidic drift ratchet capable of separating colloidal particles depending on size [72, 73]. A related system uses an artificial, asymmetric nanopore to pump ions across a membrane [74]. A recent experimental milestone is the first experimental system in which a large number of artificial Brownian motors cooperate to collectively perform macroscopic work, realized using a time-dependent magnetic field that couples to nanoscale, super-paramagnetic particles, each of which acts as a Brownian motor, and that together rotate a macroscopic sphere [75].

II. HOW TO CHARACTERIZE THE PERFORMANCE OF A BROWNIAN MOTOR

A. Characterizing macroscopic machines

The performance of macroscopic machines, such as that of cars or power drills, is well characterized by the combined concepts of *power*, *efficiency*, *torque* or *force*, and *speed*. Power is the rate at which work is done, for instance against an external force to increase the potential energy of some system, or to increase the kinetic energy of a load. Efficiency is defined as the ratio of the work output (W) to the energy supplied to the motor. For a heat engine using input heat $Q_{\rm in}$, the efficiency is thus given by $\eta = W/Q_{\rm in}$. The concepts of torque (or force) and speed supply additional information about the motor characteristics. For instance, a tractor is designed to be capable of exerting a substantial force F on an object, but only at a relatively small speed v. A small car may have the same power $P = Fv$, and may reach much higher speeds than a tractor, but only when exerting a negligible towing force on an external object.

Note that we here use the concept of a *machine*, rather than *motor*. A motor may be defined as the smallest entity capable of transforming some form of energy (such as heat, electricity, chemical energy, or radiation) into mechanical work. In contrast, a machine is usually a more complex assembly, incorporating the motor, and usually designed to perform a specific task. For instance, the difference in performance characteristics of a small car and a tractor is in part indeed due to differently designed motors, but is in part also due to the transmission system that is part of the machine.

B. Brownian machines: loose versus tight coupling

A fundamental difference between most macroscopic machines and Brownian motors lies in the nature of the coupling between the energy supply and the work output [5]. In a macroscopic com-

bustion engine, for instance, the cycle of energy supply (in the form of heat and pressure, delivered when a combustible gas is ignited in the cylinder) is tightly coupled to the work output, delivered by the moving piston. In each working cycle, compression is followed by ignition, explosion, and a 'power stroke' in a well defined manner. Random motion (for instance due to the Brownian motion of the piston) is vastly overpowered by the energies involved. Consider in contrast a single particle in the flashing ratchet of fig. 1. When the potential is switched off, a time period of free diffusion follows, which is terminated by switching the potential on. Independently of whether the switching occurs periodically or randomly, the outcome of this working cycle is statistical. If the parameters are well chosen, there is a larger-than-50% chance for the particle to end up in a minimum to the right of its starting point. In this case work of the order FL is done against the load force F. However, there is a smaller, but finite, probability that the particle performs no net motion, or even ends up in the minimum to the left, in which case the load force does work on the particle.

In other words, while the state variables of well functioning macroscopic motors are *tightly* coupled, those of Brownian motors (for instance $\Theta(t)$ and $x(t)$ in eqn. (4)) are *loosely* coupled, and a full cycle (1, 0, 1) of $\Theta(t)$ will result in a statistical distribution of $x(t)$ and of the work output W [5].

This loose coupling, and the statistical nature of their performance (as measured by position, velocity, or work output) is inherent to Brownian motors and fundamentally distinguishes them from their macroscopic counterparts. The presence of significant fluctuations in, say, the velocity also affects how well a motor can perform a certain task, and quantitative information about the fluctuations is needed for a satisfying description of the motor characteristics. In addition, as we will describe below, there is a direct relationship between velocity fluctuations and the *energy efficiency* of a Brownian motor.

C. Coherency of Brownian motors

To characterize the performance of a motor in the presence of fluctuations, consider the task of moving a cargo a certain distance within a defined time interval t. For Brownian motors, we can only know the *average* velocity of the motor for successive realisations of the process, and for a fixed time there will be a spread in the distances over which the motor carries out transport. We therefore look for a way of quantifying a motor's *coherency*.

An effective diffusion or dispersion for the motor can be defined as

$$D_{\text{eff}} = [\left\langle x^2(t) \right\rangle - \langle x(t) \rangle^2]/2t, \tag{9}$$

where the average is over an ensemble of trajectories. Ideally D_{eff} should be small, but knowing D_{eff} alone does not fully characterize the motor because it doesn't discriminate between motors with different velocities.

A coherency parameter that incorporates both velocity and spread is the Peclet number, borrowed from fluid dynamics [76], which is a measure of linear transport as compared to diffusion. The Peclet number is defined as

$$\text{Pe} = \frac{\langle v \rangle \, l}{D_{\text{eff}}}, \tag{10}$$

where l is a characteristic length, $\langle v \rangle$ is the time averaged velocity and D_{eff} is the dispersion defined as in eqn. (9). The choice of the length l in eqn. (10) is essentially arbitrary and is usually taken to be some characteristic length scale of the system. In the context of Brownian motors, the spatial period L of the ratchet potential has been used as the reference length scale l [59, 77, 78]. However, because such a choice essentially depends on the system under consideration, it is difficult to compare the performance of different types of motors. For a system-independent measure for the coherency of transporter motors, we here propose to use for l the length over which transport is being observed, $l = \langle v \rangle \, \tau$, for a fixed time interval τ. With this choice, and with the definition of D_{eff} in eqn. (9), the Peclet number becomes

$$Pe = 2\frac{l^2}{\langle \Delta x^2 \rangle}, \tag{11}$$

where l is the average distance covered by the motor during τ, and $\langle \Delta x^2 \rangle = [\langle x^2(\tau) \rangle - \langle x(\tau) \rangle^2] = 2\tau D_{\text{eff}}$ is the spread in positions at time τ averaged over many realisations of the process. This definition is in the long-time limit independent of the choice of τ, and allows comparison of the coherency of different types of transporters. A motor that will reliably cover the same distance within a time interval τ (such as a train that is always on time, with very small variations) will have a high Pe, while a less predictable (less coherent) transport system has a low Pe.

D. Efficiency

The standard definition of efficiency is given by the ratio of the output work to input energy:

$$\eta = \frac{W}{E_{\text{in}}}. \tag{12}$$

Strictly speaking, for motors operating in a constant-pressure environment, E_{in} is given by the Gibbs free energy transferred to the system [36, 79, 80]. For the flashing ratchet, E_{in} is easy to

calculate - at least in theoretical models - as the change in the potential energy of the particles during $T_{\rm on}$,

$$E_{\rm in} = \left\langle \int_0^{T_{\rm on}} \frac{{\rm d}V(x(t))}{{\rm d}x} {\rm d}x(t) \right\rangle, \tag{13}$$

where the average is over many ratchet cycles. It is then straightforward to define an efficiency for a Brownian motor based on the work performed by the motor against an external load force, F, as [80, 81]

$$\eta = \frac{F\langle v \rangle}{\dot{E}_{\rm in}}. \tag{14}$$

While this definition is unambiguous and thermodynamically correct, it is in some ways unsatisfactory for practical use, because many Brownian motors work through transport against viscous drag, without actually doing work against an external (conservative) force. However, according to eqn. (14), a motor without load force has efficiency zero.

Derényi, Bier and Astumian therefore proposed the generalized efficiency [82]

$$\eta_{\rm gen} = \frac{E_{\rm min}}{E_{\rm in}}, \tag{15}$$

where $E_{\rm min}$ is defined as the thermodynamically minumum energy required to perform the 'task' assigned to the motor. For instance, if the motor's task is to move an object of a certain size within time t over a distance l against the associated drag force $\gamma l/t$, then $E_{\rm min} = \gamma l^2/t$. If the motor performs this task in the energetically optimal way, the generalized efficiency approaches 1. If the motor's task consists of performing work W against a conservative force, then $E_{\rm min} = W$, and the generalized efficiency reduces to the definition in eqn. (14). A similar efficiency, termed the 'Stokes' efficiency, has been proposed for use in the context of chemo-mechanical energy conversion, for instance in biological motors [83].

An efficiency definition that is equivalent to that in eqn. (15) has been derived by Suzuki and Munakata [84] who considered an energy balance based on the averages of the separate terms that make up the Langevin equation without the overdamped approximation. These authors arrived at the expression

$$\eta_{\rm rec} = \frac{F\,\langle v \rangle + \gamma\,\langle v \rangle^2}{P_{\rm in}}, \tag{16}$$

where the numerator is the sum of the rate at which the motor does work against an external force, plus the power necessary to move in the long-time average at a speed $\langle v \rangle$ against a drag force

$\gamma\langle v\rangle$ through a (viscous) environment. The denominator is the average input power which can be written as

$$P_{\text{in}} = \frac{1}{\tau}\int_0^\tau \frac{\mathrm{d}V}{\mathrm{d}x}\mathrm{d}x, \tag{17}$$

for long times τ. Suzuki and Munakata explored this efficiency for flashing ratchets [84] and called it the 'rectification efficiency', expressing the fact that this definition can be also used in the absence of a bias force. That is, when the motor rectifies thermal fluctuations without doing work in the strict thermodynamical sense. Machura et al. [85] explored the rectification efficiency for rocking ratchets in the absence of a load force, and both groups of authors identified sets of design parameters that optimize the efficiency.

Eqn. (16) with the expression for the input power given in eqn. (17) is most useful for theoretical models where the exact trajectory $x(t)$ of the motor, as well as the precise potential $V(x(t))$ are known, and the input power can easily be calculated. In an experiment, this information is not normally available. Importantly, however, the average power supplied to the motor from outside must equal the motor's average power output. Suzuki and Munakata [84] made use of this insight and showed that in the long time limit the denominator in eqn. (16) can also be expressed in terms of

$$P_{\text{in}} = F\langle v\rangle + \gamma\langle v\rangle^2 + \gamma(\left\langle \Delta v^2\right\rangle - kT/m). \tag{18}$$

Here, all averages are over long times. The first and second terms are the rate at which the motor does work against an external load force F, and against the viscous drag force, respectively. The third term represents the net power dissipated by the motor to the bath due to the motor's fluctuations, and depends on the motor's (nonequilibrium) velocity fluctuations, the bath's temperature and, m, the (finite) mass of the particle undergoing transport. $\langle\Delta v^2\rangle = \langle(v-\langle v\rangle)^2\rangle$ is the time-averaged variance of the motor velocity. Using the equipartition theorem we express $kT = m\left\langle v_{\text{eq}}^2\right\rangle$ where $\left\langle v_{\text{eq}}^2\right\rangle$ is the variance of the velocity in thermal equilibrium at the bath temperature, T. We can then rewrite eqn. (16) to read

$$\eta_{\text{rec}} = \frac{F\langle v\rangle + \gamma\langle v\rangle^2}{F\langle v\rangle + \gamma\langle v\rangle^2 + \gamma(\langle\Delta v^2\rangle - \left\langle v_{\text{eq}}^2\right\rangle)}. \tag{19}$$

The third term in the denominator can be interpreted as the net heat dissipated to the bath due to velocity fluctuations [37] and is expected to be positive, as is found numerically [85].

In this spirit one can also express the energy efficiency equation (14) in terms of the variance

of the motor velocity

$$\eta = \frac{F \langle v \rangle}{F \langle v \rangle + \gamma \langle v \rangle^2 + \gamma(\langle \Delta v^2 \rangle - \left\langle v_{\rm eq}^2 \right\rangle)}. \tag{20}$$

Equations (19) and (20) potentially have tremendous practical importance. To experimentally determine the rectification efficiency, equation (19), or the energy efficiency, equation (20), of an unknown, nanoscale motor, it is sufficient to determine (i) its average velocity against a given (conservative) load force, (ii) the variance of the velocity, and (iii) the temperature of the thermal bath. As pointed out by Harada [86], this possibility represents a powerful tool for experimentalists, which to our knowledge is not generally appreciated. In addition, the relationship between fluctuations and both energy efficiency and rectification efficiency ($F = 0$) is also useful from a theoretical point of view: it provides an additional diagnostic tool when numerically 'tailoring' Brownian motors for specific performance characteristics, such as high rectification efficiency [84, 85].

Equation (20) also expresses a fundamental difference between microscopic and macroscopic motors: it is certainly not possible to determine the energy efficiency of a new car model simply by observing the average and the variance of its velocity - in addition we need detailed information about the fuel consumption. For a microscopic motor, on the other hand, we can use information about the velocity flucuations to determine the fuel comsumption.

Equations (19) and (20) were derived for the center-of-mass motion of Brownian motors without internal degrees of freedom. Clearly, for motors with internal degrees of freedom, such as protein motors, additional avenues exist for both energy dissipation and the corresponding fluctuations, and for the storage of potential energy. Equations. (19) and (20) can not be applied for such more complex situations without further evaluation. In the next section we discuss some aspects of the role of internal degrees of freedom using a specific example.

Finally we note that in our present discussion of the efficiency of Brownian motors we focused on the role of fluctuations for the motor performance, and for the energy efficiency. For a broader discussion of the energetics of Brownian motors, see the comprehensive review by Parrondo and de Cisneros in a special issue on Brownian motors [87].

III. COHERENCY AND EFFICIENCY OF A POLYMER MOTOR

In the following we discuss a Brownian motor that is based on a flashing ratchet and that possesses *internal degrees of freedom*. The basic idea is illustrated in figure 4 which shows a freely-jointed chain model of a polyelectrolyte (such as DNA in water), in which charged monomers are

separated by a distance related to the polymer's persistence length (which is about 50 nm for DNA [88, 89]). All of the polymer's degrees of freedom are activated by thermal motion, causing the polymer to continuously change its coiled shape in three dimensions. For the flashing ratchet potential, we consider a one-dimensional, asymmetric, piece-wise constant force-field (spatial average zero), that can be switched on (fig. 4, A and C) and off (B and D), creating a flashing ratchet. The spatial period L is chosen to be comparable to the dimension of the polymers random coil configuration (the radius of gyration), such that the molecule's internal degrees of freedom rearrange themselves to minimize the polymer's potential energy when the potential is on (A). When the potential is off (B), the polymer is free to approach its random coil configuration. However, each time the potential is switched on again (C) the polymer will shift its center of mass (indicated as a gray dot) to the right, inducing directed motion on average (fig. 5).

This is a relatively simple model system for a motor with active, internal degrees of freedom, and we are interested in the question of how the performance characteristics of such a system can be varied by fine-tuning of the system variables and how they compare to the performance characteristics (stall force, efficiency, Peclet number) of the extensively studied single-particle flashing ratchet.

Additional interest in such a polymer motor stems from the fact that this motor can, in principle, be realized experimentally, using colloidal DNA molecules in combination with asymmetric electrode arrays lithographically patterned onto a substrates such as silicon chips [10, 12]. In principle, a load can be attached to one end of the polymer, enabling it to perform a function similar to that of a transporter motor protein. Such an artificial motor will provide a powerful experimental system for the study of motor performance as a function of system variables, and has significant potential for applications in, for instance, lab-on-chip systems. In contrast to many other schemes for the construction of artificial molecular motors, such as most concepts to construct motors using synthetic chemistry [90] , this motor would be controllable externally (by turning on and off the electrode tracks), and power would be supplied electrically, rather than chemically.

A. Model

To model the performance of the single-molecule motor we employ a coarse grained bead-and-string model of a freely jointed polymer in which individual monomer beads represent several chemical groups and the bond length between adjacent monomers is the related Kuhn length [91]. The monomers interact via a standard simulation force field consisting of a repulsive Lennard-Jones

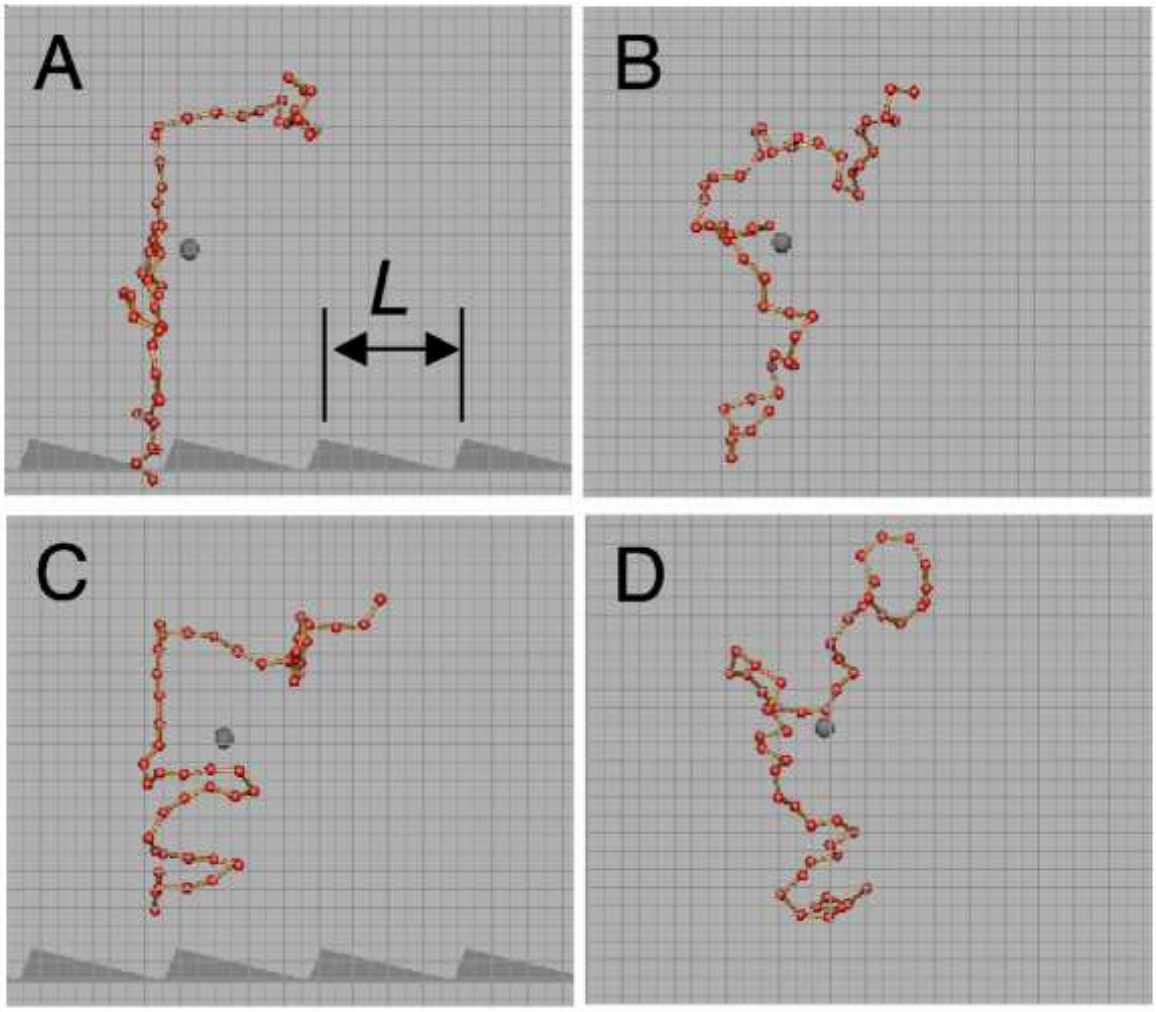

FIG. 4: Individual frames of a Brownian dynamics simulation of a single-polymer motor (for details of the simulation, please see text). The polymer is modeled as a freely jointed chain, and a one-dimensional, piece-wise linear, zero-mean force fields acts on each individual chain link. 'Flashing' of the ratchet force-field induces average forward motion of the center of mass, achieved by rectification of the thermal motion of the molecule's *internal degrees of freedom*. For an illustrative animation of this simulation, please see http://darkwing.uoregon.edu/~linkelab.

potential of the form

$$V_{ij}(r_{ij}) = \begin{cases} 4\epsilon\left((\frac{\sigma}{r_{ij}})^{12} - (\frac{\sigma}{r_{ij}})^{6}\right) + \epsilon & : \quad r_{ij} \leq 2^{\frac{1}{6}}\sigma \\ 0 & : \quad r_{ij} > 2^{\frac{1}{6}}\sigma \end{cases} \tag{21}$$

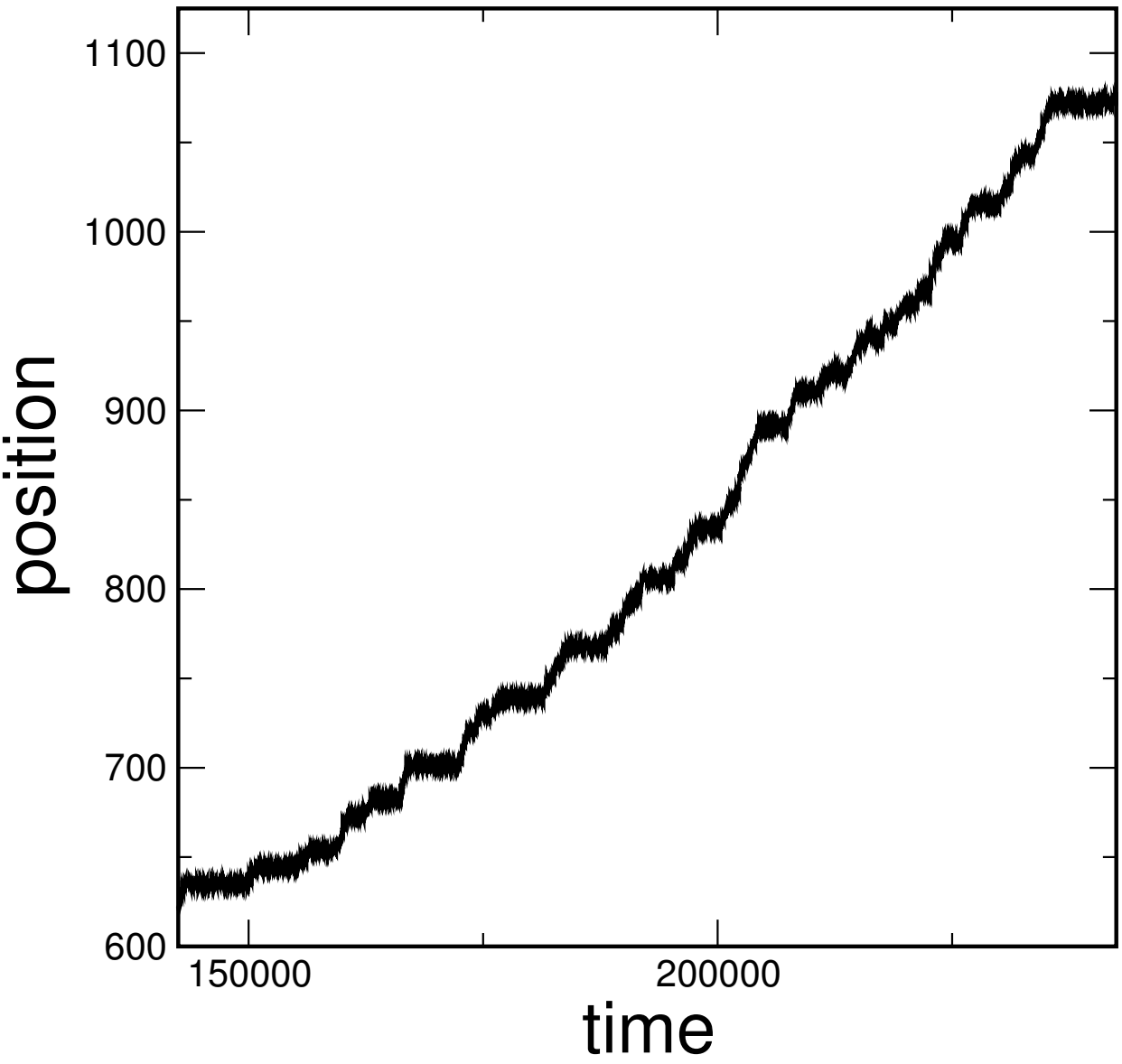

FIG. 5: Simulated data (for details, Section III A) of the center-of-mass of the single-molecular motor illustrated in fig. 4. The presence of noise is inherent to a Brownian motor.

acting between all beads. The bonds between neighboring beads on the polymer chain are modeled by a FENE potential which imposes a maximum bond extent. The functional form is

$$U(r_{ij}) = -\frac{1}{2} k_{\mathrm{F}} R_0^2 \ln\left(1 - \frac{r_{ij}^2}{R_0^2}\right), \tag{22}$$

where r_{ij} is the monomer-monomer separation and k_{F} and R_0 are the potential strength and extent parameters. The mass, m, of each bead is set to unity and we use σ, ϵ and $\tau_{\mathrm{s}} = \sqrt{m\sigma^2/\epsilon}$ to set the length, energy, and time scales. The values k_{F} and R_0 were chosen to be $30\epsilon/\sigma^2$ and 1.5σ respectively. This model of a polymer is well studied and has been used previously to model polymer

melts [92]. The equations of motion of individual beads are given by the Langevin equation:

$$m\ddot{\mathbf{r}}_i = -\gamma\dot{\mathbf{r}}_i + \xi_i(t) - \nabla V_{\rm p}(\mathbf{r}_i) - \nabla V(\mathbf{r}_i)f(t) + \mathbf{F}(\mathbf{r}_i) \tag{23}$$

where ξ_i is a random force representing the surrounding solvent and heat bath ($<\xi_i>=0; <\xi_i(t)\xi_j(t')>=2\gamma k_{\rm B}T\delta_{ij}\delta(t-t')$), γ is the friction coefficient, $V_{\rm p}$ is a sum of the internal polymer potentials given in eqns. (21) and (22), and $\mathbf{F}(\mathbf{r}_i)$ represents an external force. The above Langevin equation was simulated using Brownian dynamics [93]. In the absence of hydrodynamic interactions between the monomers this corresponds to the Rouse model of polymer dynamics.

The motor potential, $V(\mathbf{r}_i)$, is spatially periodic along one axis as shown in figure 1. $V(\mathbf{r}_i)$ is periodically 'flashed', acting to localise the polymer for a time $T_{\rm on}$ before being switched off to allow the polymer to diffuse freely for a time $T_{\rm off}$. The height of the barrier is typically set to be of the order of a few kT.

B. Results

A full description of the performance of the motor can be found in [94]. Here we highlight an example for how the motor design will determine the performance characteristics, and concentrate for this purpose on two different values of the free diffusion time $T_{\rm off}$=$10\tau_{\rm s}$ and $T_{\rm off}$=$20\tau_{\rm s}$, respectively. We fix $T_{\rm on}$= $20\tau_{\rm s}$ which we found is sufficiently long to fully localize the polymer. Further we use $V = 4kT$ and $\alpha = 0.1$. All simulations were for a total simulation time of $T = 2\times10^6\tau_{\rm s}$ using polymers of length 50 monomers. The friction coefficient, γ, was set to unity for each monomer. To calculate the effective diffusion constant as defined in eqn. (9) we split one large trajectory into sub-trajectories. In the parameter range studied here the velocity of the polymer is a product of the probability of moving forward one well while the ratchet is turned off (a decreasing function of L) with the distance gain that can be made when the polymer moves forward. The top panel in figure 6 shows the velocity of the polymer as a function of the ratchet period L. For both values of $T_{\rm off}$ studied here the maximum in velocity is similar, though the position of the peak is shifted to lower L for the shorter $T_{\rm off}$ time. This observation is in agreement with what one expects in a single-particle picture, where a shorter diffusion time $T_{\rm off}$ will yield maximum velocity for a ratchet geometry with a shorter distance over which diffusion is required.

Although the velocities of the polymer for the two cases are similar, there are differences in the behavior of the fluctuations as described in the previous section. For the longer $T_{\rm off}$, there is a greater spread in the distances travelled for different realisations of the stochastic process and

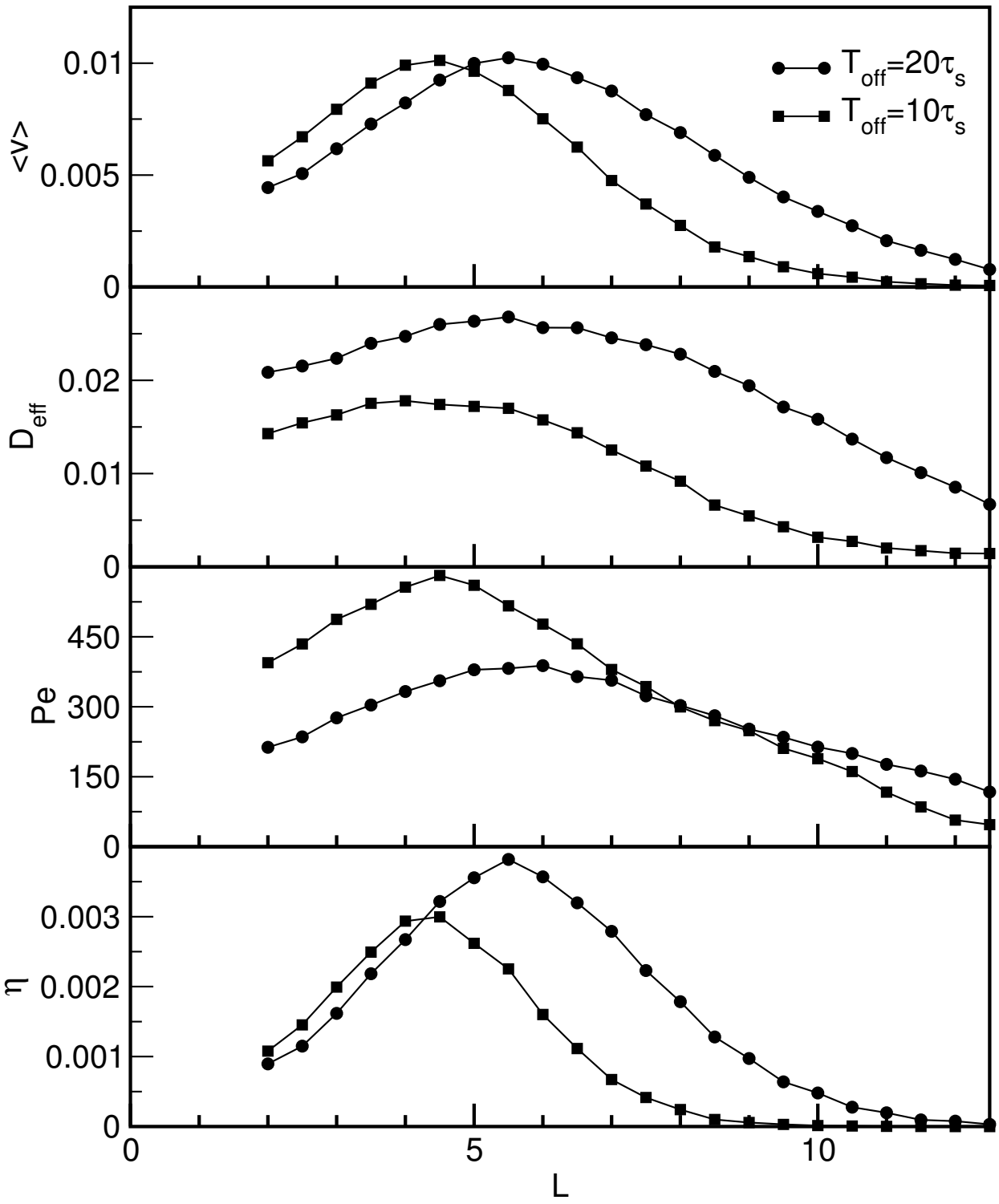

FIG. 6: Results of simulations for the motor described. From top: average velocity, dispersion $D_{\rm eff}$ as defined in eqn. (9), Peclet (10), number and efficiency (16), (Squares: $T_{\rm on} = 20\tau_{\rm s}, T_{\rm off} = 10\tau_{\rm s}$; Circles: $T_{\rm on} = 20\tau_{\rm s}, T_{\rm off} = 20\tau_{\rm s}$).

hence D_{eff} is larger. Interestingly, in both cases the maximum value of D_{eff} occurs at roughly the same L as the peak in velocity. A polymer in the abscence of a ratchet potential will diffuse with a diffusion constant $D = 0.02$. For the T_{off}=$10\tau_{\text{s}}$ case we find that $D_{\text{eff}} < D$ over the entire range of L, but D_{eff} is enhanced for T_{off}=$20\tau_{\text{s}}$ in the range where the peak in v occurs. To characterize the magnitude of velocity fluctuations with respect to the motor's average velocity, we calculate the Peclet number as defined in eqns. (10) and (11), using $l = 1000\sigma$, where σ is the monomer diameter. Note that if instead the value $l = L$ had been chosen then Pe would have been distorted towards longer lengths. As one would expect from the behavior of D_{eff}, the peak in Pe occurs at the same value of L as the peak in velocity. Importantly, however, the maximum value of Pe is substantially higher for the lower value of T_{off}, because D_{eff} is lower for the same velocity. The T_{off}= $10\tau_{\text{s}}$ motor is therefore more coherent, and is 'better suited' for on-time delivery.

The lowest panel of figure 6 shows the (rectification) efficiency as calculated using eqn. (16) for motion in the absence of an external force. First we note that the absolute values of the efficiency are quite small (order of 1% or less) compared to single-particle flashing ratchets where efficiencies of the order 5-10% are obtained [79, 84, 87]. Here we are primarily interested in the comparative efficiency of the two realizations of the polymer motor, and find that the motor with a larger Pe (T_{off}= $10\tau_{\text{s}}$) has a substantially lower efficiency than the (T_{off}= $20\tau_{\text{s}}$)-motor.

To better understand the energetics of our coupled motor system, we turn our attention to the energy balance at the single monomer level. We follow similar reasoning to Suzuki and Munakata [84], but note that due to the coupling between individual monomers, internal forces need to be considered for a motor with internal degrees of freedom. We find that the input power to a monomer with label i can be calculated using either the right or left side of the equation,

$$\frac{1}{\tau}\int_0^\tau \partial_x U_{i0}\mathrm{d}x_i = \langle v_i f_{i\text{int}}\rangle + \gamma_i \left\langle v_i^2 \right\rangle - \gamma_i kT/m_i, \tag{24}$$

where $f_{i\text{int}}$ is the instantaneous internal force acting on a monomer, and the averages are taken over time. To test this expected equality, which should be true in a long time average, we plot in figure 7 (top) the left and right hand sides of eqn. (24). The internal forces between monomers are large, leading to a relatively low signal to noise ratio, but the statistics are sufficient to show good agreement between the two ways of calculating the input energy along the entire length of the polymer. An interesting observation is that the ends of the polymer 'use' more energy than the center part. To understand this we note that when the ratchet potential is turned on, the polymer can be in an extended conformation, straddling multiple wells. When only a short segment of the polymer (usually one of the ends), occupies the adjacent well, the bulk of the polymer can pull the

segment over the potential barrier, leading to an increase in the work performed by the external field on the polymer's extremities. A more complete discussion of the performance of the polymer motors introduced here will be presented in [94].

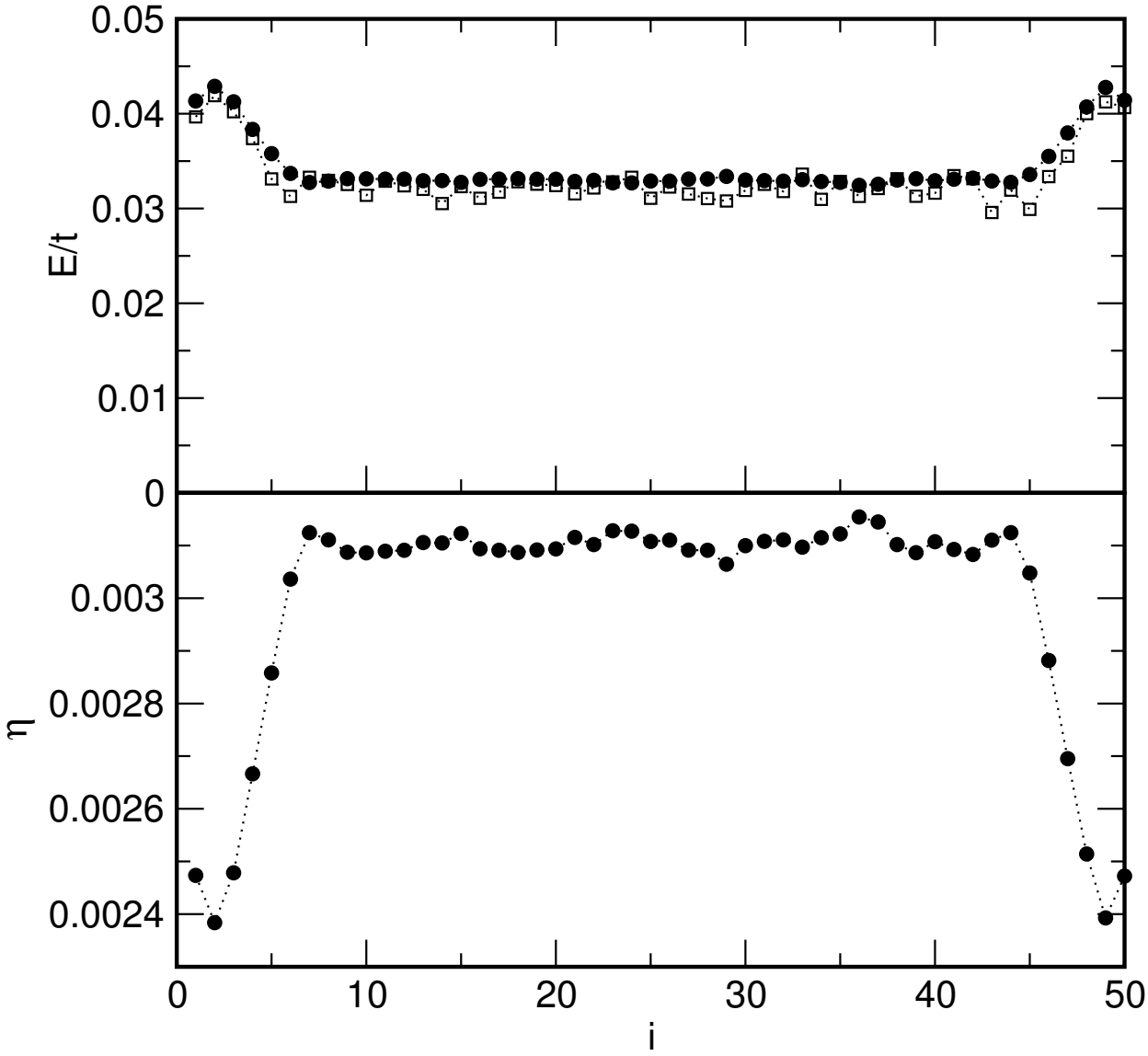

FIG. 7: Power and efficiency by monomer ($L = 4.5\sigma; T_{\rm on} = 20\tau_{\rm s}; T_{\rm off} = 10\tau_{\rm s}$). The horizontal axis i indicates the monomer label running from one to N=50. Top: Rate of energy input into the system (filled circles); rate of dissipation (open squares). Bottom: efficiency.

IV. CONCLUSIONS

In this paper we introduced the basic concepts of Brownian motors using the well-known example of a flashing ratchet. The crucial characteristic of a Brownian motor, namely the *incorporation*

of thermal motion into the motor's operational principle, not only distinguishes Brownian motors from their macroscopic counterparts, such as car engines, but also leads to richer performance characteristics. Firstly, the direction of the motor velocity is usually not straightforward to predict and often subtly depends on the choice of parameters. This property is the reason that many ratchets and Brownian motors are excellent candidates for separation devices. A second consequence of thermal fluctuations is the focus of the present paper: fluctuations are an inherent part also of the motor performance, and a full characterization of the motor performance requires characterization of the fluctuations in motor position and velocity. Crucially, the fluctuations also contain additional information. As discussed in several recent papers [84–86], a motor's velocity fluctuations contain information about the heat dissipated by the motor to the environment. Consequently it is possible to determine a motor's efficiency by simply observing the motors average velocity and the variance of the velocity [86]. We have also discussed how, for a coupled motor, the internal degrees of freedom need to be taken into account.

---

[1] P. Hänggi and R. Bartussek, Lect. Note. Phys. **476**, 294 (1996).

[2] R. D. Astumian, Science **276**, 917 (1997).

[3] R. D. Astumian and P. Hänggi, Physics Today **55**, (11) 33 (2002).

[4] P. Reimann, Physics Reports **361**, 57 (2002).

[5] P. Reimann and P. Hänggi, Appl. Phys. A **75**, 169 (2002).

[6] A. L. R. Bug and B. J. Berne, Phys. Rev. Lett. **59**, 948 (1987).

[7] A. Ajdari and J. Prost, C.R. Acad. Sci. Paris, Série II **315**, 1635 (1992).

[8] J. Prost, J. F. Chauwin, L. Peliti, and A. Ajdari, Phys. Rev. Lett. **72**, 2652 (1994).

[9] J. Rousselet, L. Salome, A. Ajdari, and J. Prost, Nature **370**, 446 (1994).

[10] R. W. Hammond, J. S. Bader, S. A. Henck, M. W. Deem, G. A. McDermott, J. M. Bustillo, and J. M. Rothberg, Electrophoresis **21**, 74 (2000).

[11] J. S. Bader, M. W. Deem, R. W. Hammond, S. A. Henck, J. W. Simpson, and J. M. Rothberg, Appl. Phys. A **75**, 275 (2002).

[12] J. S. Bader, R. W. Hammond, S. A. Henck, M. W. Deem, G. A. McDermott, J. M. Bustillo, J. W. Simpson, G. T. Mulhern, and J. M. Rothberg, Proc. Natl. Acad. Sci. **96**, 13165 (1999).

[13] F. Falo, P. J. Martinez, J. J. Mazo, and S. Cilla, Europhys. Lett. **45**, 700 (1999).

[14] S. Weiss, D. Koelle, J. Muller, R. Gross, and K. Barthel, Europhys. Lett. **51**, 499 (2000).

[15] T. Orlando, K. Segall, J. Mazo, and F. Falo (2002), APS March Meeting.

[16] J. B. Majer, J. Peguiron, M. Grifoni, M. Tusveld, and J. E. Mooij, Phys. Rev. Lett. **90**, 056802 (2003).

[17] C. S. Lee, B. Janko, I. Derényi, and A. L. Barabasi, Nature **400**, 337 (1999).

[18] S. Savel'ev and F. Nori, Nature Materials **1**, 179 (2002).

[19] J. E. Villegas, S. Savel'ev, F. Nori, E. M. Gonzalez, J. V. Anguita, R. Garcia, and J. L. Vicent, Science **302**, 1188 (2003).

[20] A. V. Chaplik, Sov. Phys. JETP **33**, 997 (1971).

[21] G. F. Giuliani and J. J. Quinn, Phys. Rev. B **26**, 4421 (1982).

[22] B. L. Altshuler, A. G. Aronov, and D. E. Khmelnitsky, J. Phys. C **15**, 7367 (1982).

[23] J. B. Johnson, Phys. Rev. **32**, 97 (1928).

[24] H. Nyquist, Phys. Rev. **32**, 110 (1928).

[25] Callen H. B. and T. A. Welton, Phys. Rev. **83**, 34 (1951).

[26] R. Ketzmerick, M. Weiss, and F.-J. Elmer (1998), http://monet.physik.unibas.ch/∼elmer/bm.

[27] P. Reimann, R. Bartussek, R. Haussler, and P. Hänggi, Phys. Lett. A **215**, 26 (1996).

[28] R. Eichhorn, P. Reimann, and P. Hänggi, Phys. Rev. Lett. **88**, 190601 (2002); *ibid.* Phys. Rev. E, **66**, 066132 (2002).

[29] R. Eichhorn and P. Reimann, Phys. Rev. E **70**, 035106 (2004).

[30] M. E. Fisher and A. B. Kolomeisky, Proc. Natl. Acad. Sci. USA **96**, 6597 (1999).

[31] R. D. Vale and R. A. Milliagan, Science **288**, 89 (2000).

[32] K. Svoboda, C. F. Schmidt, B. J. Schnapp, and S. M. Block, Nature **365**, 721 (1993).

[33] K. Kitamura, M. Tokunaga, H. I. Atsuko, and T. Yanagida, Nature **397**, 129 (1999).

[34] A. Yildiz, J. N. Forkey, S. A. McKinney, T. Ha, Y. E. Goldman, and P. R. Selvin, Science **300**, 2061 (2003).

[35] A. Yildiz, M. Tomishige, R. D. Vale, and P. R. Selvin, Science **303**, 676 (2004).

[36] F. Jülicher, A. Ajdari, and J. Prost, Rev. Mod. Phys. **69**, 1269 (1997).

[37] H. Wang and G. Oster, Appl. Phys. A **75**, 315 (2002).

[38] P. Hänggi, R. Bartussek, P. Talkner, and J. Luczka, Europhys. Lett. **35**, 315 (1996).

[39] P. Hänggi, F. Marchesoni, and F. Nori, Ann. Physik. (Leipzig) **15**, xxxx (2005), cond-mat/0410033.

[40] F. Jülicher and J. Prost, Phys. Rev. Lett. **75**, 2618 (1995).

[41] P. Reimann, R. Kawai, C. van den Broeck, and P. Hänggi, Europhys. Lett. **45**, 545 (1999).

[42] S. Savel'ev, F. Marchesoni, and F. Nori, Phys. Rev. Lett. **91**, 010601 (2003).

[43] R. Bartussek and P. Hänggi, Phys. Bl. **51**, 506 (1995).

[44] P. Jung, J. G. Kissner, and P. Hänggi, Phys. Rev. Lett. **76**, 3436 (1996).

[45] J. L. Mateos, Phys. Rev. Lett. **84**, 258 (2000).

[46] H. Schanz, M. F. Otto, R. Ketzmerick, and T. Dittrich, Phys. Rev. Lett **87**, 070601 (2001).

[47] R. Bartussek, P. Hänggi, and J. G. Kissner, Europhys. Lett. **28**, 459 (1994).

[48] J. Luczka, R. Bartussek, and P. Hänggi, Europhys. Lett. **31**, 431 (1995).

[49] I. Zapata, R. Bartussek, F. Sols, and P. Hänggi, Phys. Rev. Lett. **77**, 2292 (1996).

[50] P. Reimann, M. Grifoni, and P. Hänggi, Phys. Rev. Lett. **79**, 10 (1997).

[51] I. Goychuk, M. Grifoni, and P. Hänggi, Phys. Rev. Lett. **81**, 649 (1998); *ibid*, Phys. Rev. Lett. **81**, 2837

(1998).

[52] M. Grifoni, M. S. Ferreira, J. Peguiron, and J. B. Majer, Phys. Rev. Lett. **89**, 146801 (2002).

[53] J. Lehmann, S. Kohler, P. Hänggi, and A. Nitzan, Phys. Rev. Lett. **88**, 228305 (2002).

[54] H. Linke, T. E. Humphrey, A. Löfgren, O. Sushkov, R. Newbury, R. P. Taylor, and P. Omling, Science **286**, 2314 (1999).

[55] R. D. Astumian and I. Derényi, Biophys. J. **77**, 993 (1999).

[56] R. D. Astumian and M. Bier, Biophys. J. **70**, 637 (1996).

[57] I. Derényi and T. Vicsek, Phys. Rev. Lett. **75**, 374 (1995).

[58] Z. Csahok, F. Family, and T. Vicsek, Phys. Rev. E **55**, 5179 (1997).

[59] D. Dan and A. M. Jaynnavar, Phys. Rev. E **66**, 41106 (2002).

[60] B. Cleuren and C. van den Broeck, Europhys. Lett. **54**, 1 (2001).

[61] J. Buceta, J. M. R. Parrondo, C. van den Broeck, and F. J. de la Rubia, Phys. Rev. E **61**, 6287 (2000).

[62] C. van den Broeck, I. Bena, P. Reimann, and J. Lehmann, Ann. Physik **9**, 713 (2000).

[63] S. E. Mangioni, R. R. Deza, and H. S. Wio, Phys. Rev. E **63**, 041115 (2001).

[64] H. Linke, ed., *Ratchets and Brownian Motors: Basics, Experiments and Applications*, vol. 75 (2) of *Appl. Phys. A* (2002), p. 167-352.

[65] L. Faucheux, L. Bourdieu, P. Kaplan, and A. Libchaber, Phys. Rev. Lett. **74**, 1504 (1995).

[66] A. M. Song, A. Lorke, A. Kriele, J. P. Kotthaus, W. Wegscheider, and M. Bichler, Phys. Rev. Lett. **80**, 3831 (1998).

[67] H. Linke, W. Sheng, A. Löfgren, H. Xu, P. Omling, and P. E. Lindelof, Europhys. Lett. **44**, 341 (1998).

[68] A. M. Song, P. Omling, L. Samuelson, W. Seifert, and I. Shorubalku, Appl. Phys. Lett. (2001).

[69] T. E. Humphrey, R. Newbury, R. P. Taylor, and H. Linke, Phys. Rev. Lett. **89**, 11680 (2002).

[70] T. E. Humphrey and H. Linke (2004), cond-mat/0401377.

[71] T. E. Humphrey and H. Linke (2004), cond-mat/0407509.

[72] C. Kettner, P. Reimann, P. Hänggi, and F. Muller, Phys. Rev. E **61**, 312 (2000).

[73] S. Matthias and F. Muller, Nature **424**, 53 (2003).

[74] Z. Siwy and A. Fuliński, Phys. Rev. Lett. **89**, 198103 (2002).

[75] A. Engel, H. W. Müller, P. Reimann, and A. Jung, Phys. Rev. Lett. **91**, 060602 (2003).

[76] L. D. Landau and E. M. Lifshitz, *Fluid Mechanics* (Pergamon Press, New York, 1959), p. 203.

[77] J. A. Freund and L. Schimansky-Geier, Phys. Rev. E **60**, 1304 (1999).

[78] B. Linder and L. Schimansky-Geier, Phys. Rev. Lett. **89**, 230602 (2002).

[79] J. M. R. Parrondo, J. M. Blanco, F. J. Cao, and R. Brito, Europhys. Lett. **43**, 248 (1998).

[80] H.-X. Zhou and Y. Chen, Phys. Rev. Lett. **77**, 194 (1996).

[81] K. Sekimoto, J. Phys. Soc. Jpn. **66**, 1234 (1997).

[82] I. Derényi, M. Bier, and R. D. Astumian, Phys. Rev. Lett. **83**, 903 (1999).

[83] H. Wang and G. Oster, Europhys. Lett. **57**, 131 (2002).

[84] D. Suzuki and T. Munakata, Phys. Rev. E **68**, 021906 (2003).

[85] L. Machura, M. Kostur, P. Talkner, J. Łuczka, F. Marchesoni, and P. Hänggi, Phys. Rev. E **70**, 061105 (2004).

[86] T. Harada (2003), cond-mat/0310547.

[87] J. M. R. Parrondo and B. de Cisneros, Appl. Phys. A. **75**, 179 (2002).

[88] A. Y. Grosberg and A. R. Khokhlov, *Giant Molecules, Here, There and Everywhere* (Academic Press, San Diego, CA, 1997).

[89] J. Howard, *Mechanics of Motor Proteins and the Cytoskeleton* (Sinauer, Sunderland, Massachusetts, 2001).

[90] V. Balzani, A. Credi, F. Raymo, and J. F. Stoddart, Angew. Chem. Int. Ed. **39**, 3348 (2000).

[91] M. Doi and S. F. Edwards, *The Theory of Polymer Dynamics* (Oxford University Press, Oxford, 1986).

[92] K. Kremer and G. S. Grest, J. Chem. Phys. **92**, 5057 (1990).

[93] W. F. van Gunsteren and H. J. C. Berensden, Mol. Phys. **45**, 637 (1982).

[94] M. T. Downton, M. J. Zuckermann, E. M. Craig, M. Plischke, and H. Linke (2005), in preparation.